Karlsruher Institut für Technologie

Karlsruhe Reports in Informatics 2012,16
Edited by Karlsruhe Institute of Technology,
Faculty of Informatics
ISSN 2190-4782

Generalized Catmull-Clark Subdivision

Qi Chen and Hartmut Prautzsch

2012

KIT – University of the State of Baden-Wuerttemberg and National
Research Center of the Helmholtz Association

Fakultät für **Informatik**

Generalized Catmull-Clark Subdivision

Qi Chen and Hartmut Prautzsch
Karlsruhe Institute of Technology, Germany
chenqi@ira.uka.de and prautzsch@kit.edu

August 8, 2012

Abstract

The Catmull-Clark subdivision algorithm consists of an operator that can be decomposed into a refinement operator and a successively executed smoothing operator, where the refinement operator splits each face with m vertices into m quadrilateral subfaces and the smoothing operator replaces each internal vertex with an affine combination of its neighboring vertices and itself. Over regular meshes, this smoothing operator is identical to applying the (face-)midpoint operator twice, where each application of the midpoint operator maps a mesh to the dual mesh that connects the centers of adjacent faces.

In this paper, we generalize the Catmull-Clark scheme by generalizing the smoothing operator on regular meshes and by combining several smoothing operations into one subdivision step. The generalized Catmull-Clark subdivision operators build an infinite class of quadrilateral subdivision schemes, which includes the Catmull-Clark scheme with restricted parameters and the midpoint schemes.

We analyze the smoothness of the resulting subdivision surfaces at regular and at extraordinary points by estimating the norm of a second order difference scheme and by using established methods for analyzing midpoint subdivision. The surfaces are smooth for regular meshes and they are also smooth at extraordinary points for most generalized Catmull-Clark subdivision schemes.

Categories and Subject Descriptors (according to ACM CCS): I.3.5 [Computer Graphics]: Computational Geometry and Object Modeling — Curve, surface, solid, and object representations

Keywords: subdivision surfaces; Catmull-Clark subdivision algorithm; midpoint subdivision; difference schemes; extraordinary points; characteristic map

1 Introduction

When applying the Lane-Riesenfeld subdivision algorithm [LR80] to regular 2-dimensional quadrilateral manifold meshes, the limiting surfaces are uniform B-spline surfaces. Midpoint subdivision generalizes Lane-Riesenfeld subdivision in so far as it can be applied to arbitrary 2-dimensional quadrilateral manifold meshes. A midpoint subdivision scheme consists of an operator $M_n = A^{n-1}R$ of degree $n \in \mathbb{N}$, which is used successively to subdivide an input mesh $\mathcal{M}$. The *refinement operator* R maps $\mathcal{M}$ to the quadrilateral mesh $R\mathcal{M}$, where the edges of $R\mathcal{M}$ connect the center with all edge midpoints for each face of $\mathcal{M}$ and any vertex of $\mathcal{M}$ with all adjacent edge midpoints as shown at the top of Figure 1.1. The *averaging operator* A maps $\mathcal{M}$ to the dual mesh $A\mathcal{M}$ that connects the centers of adjacent faces as shown at the bottom of Figure 1.1.

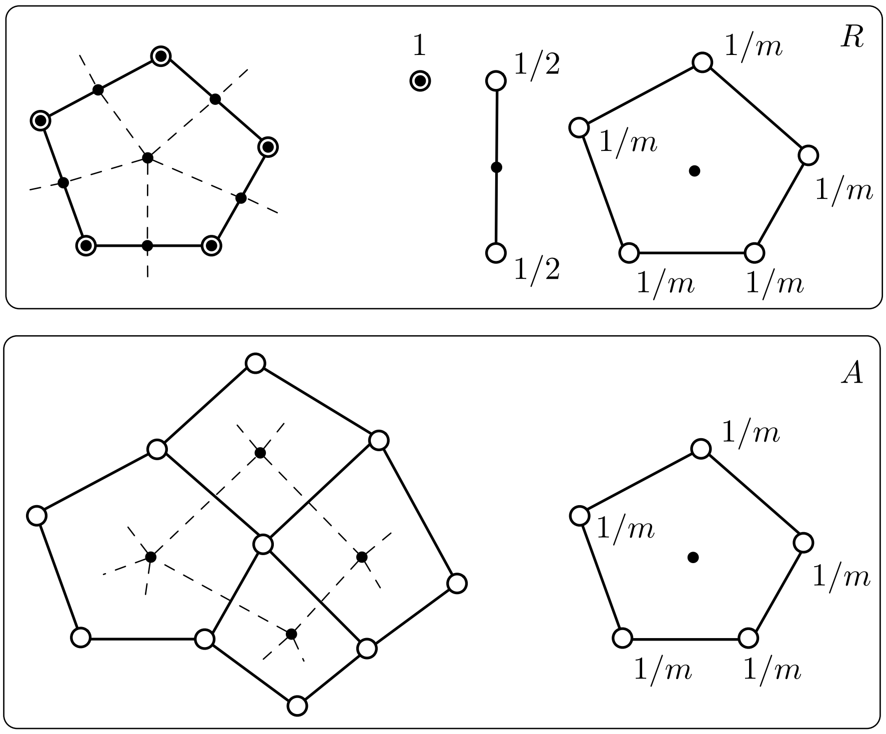

Figure 1.1: Two basic operators for subdividing quadrilateral meshes, where m is the valence of a vertex or face: refinement operator R (top) and averaging operator A (bottom).

For arbitrary meshes, the midpoint scheme of degree 2 or 3 is Doo-Sabin or Catmull-Clark subdivision [DS78, CC78] with specific parameters, respectively. The limiting surfaces generated by these schemes are smooth everywhere as shown e. g. in [PR98], where Reif's C^1-criterion [Rei95] was used and the spectral properties of the subdivision matrix were numerically analyzed. Numerically computing or estimating the spectral properties of the subdivision matrix is a bottleneck when Reif's C^1-criterion is used to analyze infinite classes of subdivision schemes. Therefore, the C^1 result of midpoint subdivision was merely extended by [ZS01] up to degree 9 and only recently, further geometric arguments were developed that helped to prove that midpoint subdivision for any degree $n \geq 2$ generates C^1 subdivision surfaces everywhere [PC11].

The Catmull-Clark scheme consists of an operator whose masks are shown in Figure 1.2 and this operator can be decomposed into a refinement operator R (see Figure 1.1, top) and a successively executed smoothing operator $B_{\alpha,\beta}$ with constraints $\alpha(4) = 1/4$ and $\beta(4) = 1/2$ and with the following relationships

$$\tilde{\alpha} = \alpha + \frac{\beta}{2} + \frac{\gamma}{4}, \quad \tilde{\beta} = \frac{\beta}{2} + \frac{\gamma}{2}, \quad \text{and} \quad \tilde{\gamma} = \frac{\gamma}{4}\,.$$

The smoothing operator $B_{\alpha,\beta}$ maps a mesh $\mathcal{M}$ to the quadrilateral mesh $B_{\alpha,\beta}\mathcal{M}$, where each internal vertex in $\mathcal{M}$ is replaced with an affine combination of its neighboring vertices and itself, see Figure 1.3. Over regular meshes, since $\alpha(4) = 1/4$ and $\beta(4) = 1/2$, $B_{\alpha,\beta}$ is identical to two applications of the (face-)midpoint operator A.

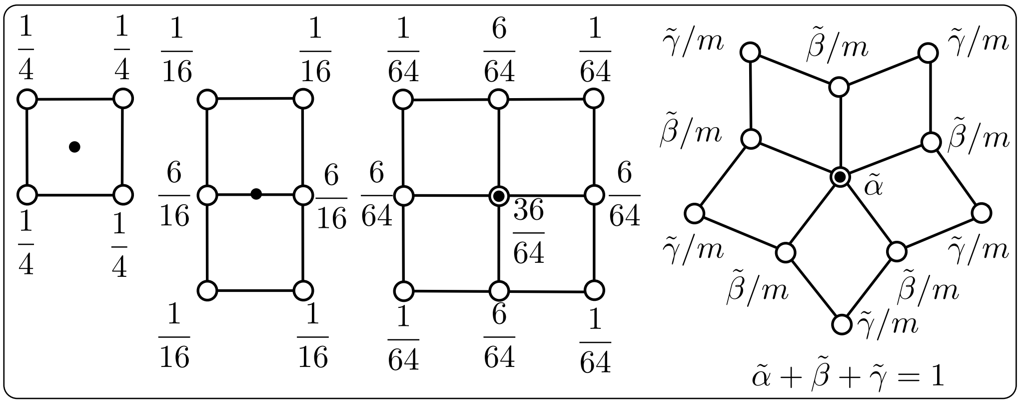

Figure 1.2: Masks for the Catmull-Clark scheme, where the left three masks are for new regular vertices and the right is for new extraordinary vertices with valence $m(\neq 4)$. In [CC78], Catmull and Clark suggest $\tilde{\alpha} = 1 - \frac{7}{4m}$, $\tilde{\beta} = \frac{3}{2m}$, and $\tilde{\gamma} = \frac{1}{4m}$.

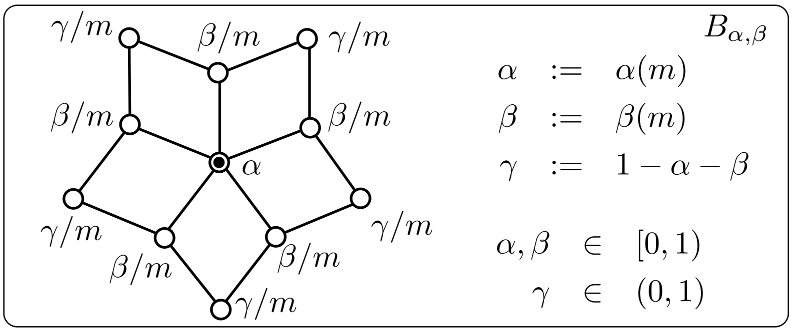

Figure 1.3: Smoothing operator $B_{\alpha,\beta}$ for a vertex of valence m.

In this paper, we generalize the Catmull-Clark scheme in two ways. First, we generalize the smoothing operator on regular meshes. Second, we execute several smoothing operations, which may have different parameters, in one subdivision step. The generalized Catmull-Clark subdivision operators build an infinite class of quadrilateral subdivision schemes, which includes the Catmull-Clark scheme with restricted parameters and the midpoint schemes.

We further develop the techniques used in [PC11] to analyze the smoothness of the resulting subdivision surfaces. The surfaces are smooth for regular meshes and they are also smooth at their extraordinary points for most generalized Catmull-Clark subdivision schemes.

2 Generalized Catmull-Clark subdivision

In this section, we define a *generalized Catmull-Clark scheme* $\overline{M}_n$ of degree $n \geq 2$ by

$$\overline{M}_n = \begin{cases} B_r \cdots B_1 R & , \quad \text{if } n = 2r+1 \\ AB_r \cdots B_1 R & , \quad \text{if } n = 2r+2 \end{cases},$$

where R and A are the refinement operator and the averaging operator respectively, as shown in Figure 1.1, and $B_i = B_{\alpha_i,\beta_i}$ are smoothing operators, as shown in Figure 1.3. The functions $\alpha_i(\cdot)$ and $\beta_i(\cdot)$ are non-negative functions depending on i and they satisfy $0 < \alpha_i + \beta_i < 1$ for all i.

If $\alpha_1(4) = 1/4$ and $\beta_1(4) = 1/2$, then $B_1 = A^2$ on regular meshes and $\overline{M}_3 = B_1 R$ is the Catmull-Clark scheme with restricted parameters α_1 and β_1, i. e., at extraordinary points with valencies $m(\neq 4)$, α_1 and β_1 satisfy $\alpha_1(m), \beta_1(m) \in [0, 1)$ and $\alpha_1(m) + \beta_1(m) \in (0, 1)$.

If $\alpha_1 \equiv 1/4$ and $\beta_1 \equiv 1/2$, then $B_1 = A^2$ on arbitrary meshes and $\overline{M}_n = AB_1^r R$ or $\overline{M}_n = B_1^r R$ are midpoint schemes M_n of degree n if n is even or odd, respectively.

In the following sections, we analyze the smoothness property of generalized Catmull-Clark subdivision surfaces at their regular points and also at their extraordinary points.

3 Smoothness for regular meshes

To analyze the smoothness of generalized Catmull-Clark schemes for regular meshes, we introduce a second order difference scheme and analyze its norm in this section.

A regular quadrilateral mesh $\mathcal{C}$ can be represented by the biinfinite matrix $\mathcal{C} = [\mathbf{c_i}]_{\mathbf{i}\in\mathbb{Z}^2}$ of its vertices $\mathbf{c_i}$, which are connected by the edges $\mathbf{c_j c_{j+e_\mathit{k}}}$, $\mathbf{j} \in \mathbb{Z}^2, k = 1, 2$, as shown in Figure 3.1, where

$$[\mathbf{e}_1\ \mathbf{e}_2] = \begin{bmatrix} 1 & 0 \\ 0 & 1 \end{bmatrix} .$$

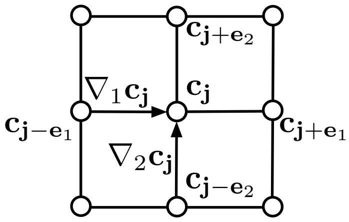

Figure 3.1: A subnet of a regular quadrilateral mesh.

To analyze smoothness, we need the (backward) differences

$$\begin{aligned} \nabla_k \mathbf{c_i} &= \mathbf{c_i} - \mathbf{c_{i-e_\mathit{k}}} , \quad k = 1, 2, \\ \nabla \mathbf{c_i} &= [\nabla_1 \mathbf{c_i}\ \nabla_2 \mathbf{c_i}] , \\ \nabla\nabla \mathbf{c_i} &= \nabla(\nabla \mathbf{c_i}) = [\nabla_1\nabla_1 \mathbf{c_i}\ \nabla_1\nabla_2 \mathbf{c_i}\ \nabla_2\nabla_1 \mathbf{c_i}\ \nabla_2\nabla_2 \mathbf{c_i}] , \end{aligned}$$

and the mesh $\mathcal{C}_{\nabla\nabla} = [\nabla\nabla\mathbf{c_i}]_{\mathbf{i}\in\mathbb{Z}^2}$ of the second order differences $\nabla\nabla\mathbf{c_i}$.

Let U be A, R, or B_i. Since U maps a linear mesh $[l(\mathbf{i})]_{\mathbf{i}\in\mathbb{Z}^2}$ to itself, where $l : \mathbb{R}^2 \to \mathbb{R}$ is any linear function, a second order difference scheme $U_{\nabla\nabla}$ exists such that

$$(U\mathcal{C})_{\nabla\nabla} = U_{\nabla\nabla}\mathcal{C}_{\nabla\nabla} \tag{3.1}$$

for all meshes $\mathcal{C}$, see [Kob00, Equations (11) and (12)].

Over regular quadrilateral meshes, we restrict $\alpha(m)$ and $\beta(m)$ to the valence $m = 4$ and consider α and β to be constants in this section.

Applying a generalized Catmull-Clark subdivision operator

$$U = B_r \cdots B_1 R \quad \text{or} \quad U = AB_r \cdots B_1 R$$

to the grid $\mathbb{Z}^2$, we obtain the scaled grid $\mathbb{Z}^2 / 2$. We recall the following well-known fact, which can be derived easily from [Dyn92, Theorem 7.6 on Page 93].

Theorem 3.1. **(C^1 condition for regular meshes)**
Let

$$\|\mathcal{C}\|_\infty := \sup_{\mathbf{i}\in\mathbb{Z}^2} \|\mathbf{c}_\mathbf{i}\| \quad \textit{and} \quad \|U\| := \sup_{\|\mathcal{C}\|_\infty=1} \|U\mathcal{C}\|_\infty .$$

If U maps $\mathbb{Z}^2$ to $\mathbb{Z}^2 / 2$ and if $2\,U_{\nabla\nabla}$ has some contractive power, i. e., if

$$\|U^k_{\nabla\nabla}\| < 1/2^k$$

*for some k, then U is a C^1-*scheme, *i. e., for any bounded mesh $\mathcal{C}$ there is a continuously differentiable function $\mathbf{f}(x, y)$ such that*

$$\lim_{k\to\infty} \|U^k\mathcal{C} - \mathbf{f}(\mathbb{Z}^2 / 2^k)\| = 0 .$$

To check the prerequisites of this theorem, we use

Lemma 3.2. (Estimates for three second difference schemes)

(a) $\|(B_{\alpha,\beta})_{\nabla\nabla}\| = 1$ *for* $\alpha,\ \beta,\ 1-\alpha-\beta \in [0, 1]$,

(b) $\|A_{\nabla\nabla}\| = 1$, *and*

(c) $\|(B_{\alpha,\beta}R)_{\nabla\nabla}\| \le \max\left\{\frac{2\alpha+\beta}{4},\ \frac{1}{2} - \frac{2\alpha+\beta}{4}\right\} < \frac{1}{2}$ *for* $\alpha,\ \beta \in [0, 1)$ *and* $1-\alpha-\beta \in (0, 1)$.

Proof. Since $(B_{\alpha,\beta})_{\nabla\nabla} = B_{\alpha,\beta}$ and $\|B_{\alpha,\beta}\| = 1$ for $\alpha,\ \beta,\ 1-\alpha-\beta \in [0, 1]$, we get (a).

Since $A_{\nabla\nabla} = A$ and $\|A\| = 1$, (b) follows.

Figure 3.2 shows the meshes $\mathcal{C}$ and $B_{\alpha,\beta}R\,\mathcal{C}$ schematically. We calculate the second differences in these meshes and get

$$\begin{aligned}
\nabla_1^2\mathbf{b}_{52} &= \frac{\beta}{16}(\nabla_1^2\mathbf{c}_{30} + \nabla_1^2\mathbf{c}_{32}) + \frac{4\alpha+\beta}{8}\nabla_1^2\mathbf{c}_{31}, \\
\nabla_1^2\mathbf{b}_{42} &= \frac{\gamma}{16}(\nabla_1^2\mathbf{c}_{20} + \nabla_1^2\mathbf{c}_{30} + \nabla_1^2\mathbf{c}_{22} + \nabla_1^2\mathbf{c}_{32}) + \frac{\beta+\gamma}{8}(\nabla_1^2\mathbf{c}_{21} + \nabla_1^2\mathbf{c}_{31}), \\
\nabla_1^2\mathbf{b}_{51} &= \frac{2\alpha+\beta}{8}(\nabla_1^2\mathbf{c}_{30} + \nabla_1^2\mathbf{c}_{31})\ , \\
\nabla_1^2\mathbf{b}_{41} &= \frac{\beta+2\gamma}{16}(\nabla_1^2\mathbf{c}_{20} + \nabla_1^2\mathbf{c}_{30} + \nabla_1^2\mathbf{c}_{21} + \nabla_1^2\mathbf{c}_{31})\ , \quad \text{and} \\
\nabla_2\nabla_1\mathbf{b}_{52} &= \frac{4\alpha+2\beta+\gamma}{16}\nabla_2\nabla_1\mathbf{c}_{31} + \frac{\beta+\gamma}{16}(\nabla_2\nabla_1\mathbf{c}_{21} + \nabla_2\nabla_1\mathbf{c}_{32}) \\
&\quad + \frac{\gamma}{16}\nabla_2\nabla_1\mathbf{c}_{22}\ .
\end{aligned}$$

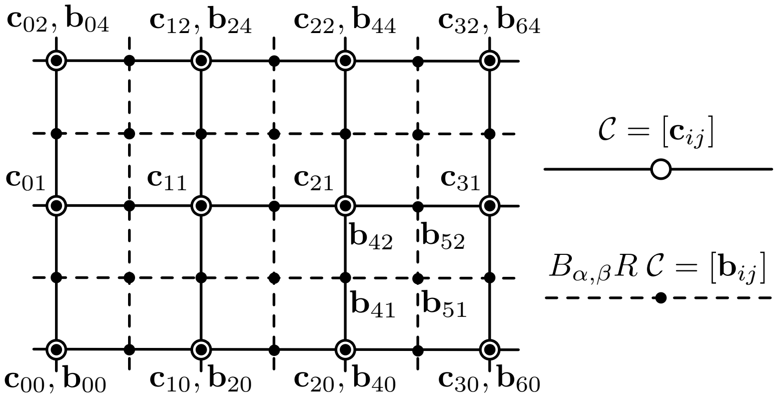

Figure 3.2: A pair of meshes $\mathcal{C}$ and $B_{\alpha,\beta} R\, \mathcal{C}$.

Similarly, we can derive such equalities for all other elements in $(B_{\alpha,\beta}R)_{\nabla\nabla}\, \mathcal{C}_{\nabla\nabla}$, where $\gamma = 1 - \alpha - \beta \in (0,1)$. Thus, since $\alpha, \beta \in [0,1)$, we get

$$
\begin{aligned}
& \|(B_{\alpha,\beta}R)_{\nabla\nabla}\| \\
\leq\ & \max\left\{2 \cdot \frac{\beta}{16} + \frac{4\alpha+\beta}{8},\ 4 \cdot \frac{\gamma}{16} + 2 \cdot \frac{\beta+\gamma}{8},\ 2 \cdot \frac{2\alpha+\beta}{8},\right. \\
& \qquad \left. 4 \cdot \frac{\beta+2\gamma}{16},\ \frac{4\alpha+2\beta+\gamma}{16} + 2 \cdot \frac{\beta+\gamma}{16} + \frac{\gamma}{16}\right\} \\
=\ & \max\left\{\frac{2\alpha+\beta}{4},\ \frac{\beta+2\gamma}{4},\ \frac{\alpha+\beta+\gamma}{4}\right\} \\
=\ & \max\left\{\frac{2\alpha+\beta}{4},\ \frac{1}{2} - \frac{2\alpha+\beta}{4}\right\} \\
=\ & \max\left\{\frac{\alpha}{4} + \frac{1-\gamma}{4},\ \frac{1}{2} - \left(\frac{\alpha}{4} + \frac{1-\gamma}{4}\right)\right\} < \frac{1}{2}\,.
\end{aligned}
$$

This proves (c). $\square$

Theorem 3.3. **(C^1 continuity for regular meshes)**
Any generalized Catmull-Clark scheme is a C^1-scheme for regular meshes.

Proof. Let $U = B_r \cdots B_1 R$ or $U = AB_r \cdots B_1 R$ be a generalized Catmull-Clark operator. Using Equation (3.1) and Lemma 3.2, we obtain

$$
\begin{aligned}
& \|U_{\nabla\nabla}\| \\
\leq\ & \begin{cases} \|(B_r)_{\nabla\nabla}\| \cdots \|(B_2)_{\nabla\nabla}\| \|(B_1R)_{\nabla\nabla}\|\,, \text{if } U = B_r \cdots B_1 R \\ \|A_{\nabla\nabla}\| \|(B_r)_{\nabla\nabla}\| \cdots \|(B_2)_{\nabla\nabla}\| \|(B_1R)_{\nabla\nabla}\|\,, \text{if } U = AB_r \cdots B_1 R \end{cases} \\
\leq\ & \|(B_1R)_{\nabla\nabla}\| \leq \max\left\{\frac{2\alpha_1+\beta_1}{4},\ \frac{1}{2} - \frac{2\alpha_1+\beta_1}{4}\right\} < \frac{1}{2}\,.
\end{aligned}
$$

Since U maps $\mathbb{Z}^2$ to $\mathbb{Z}^2/2$, we conclude from Theorem 3.1 that U is a C^1-scheme. $\square$

4 Basic observations

In this section, we consider generalized Catmull-Clark subdivision for arbitrary quadrilateral meshes with extraordinary vertices. Interior vertices or faces of a quadrilateral mesh are called *extraordinary* if their valence does not equal 4.

Subdividing by R, $B_{\alpha,\beta}$, and A does not increase the number of extraordinary elements and isolates these elements. Therefore, it suffices to consider only (sub)meshes with one extraordinary vertex, as illustrated in Figure 4.1. These meshes are called *ringnets*.

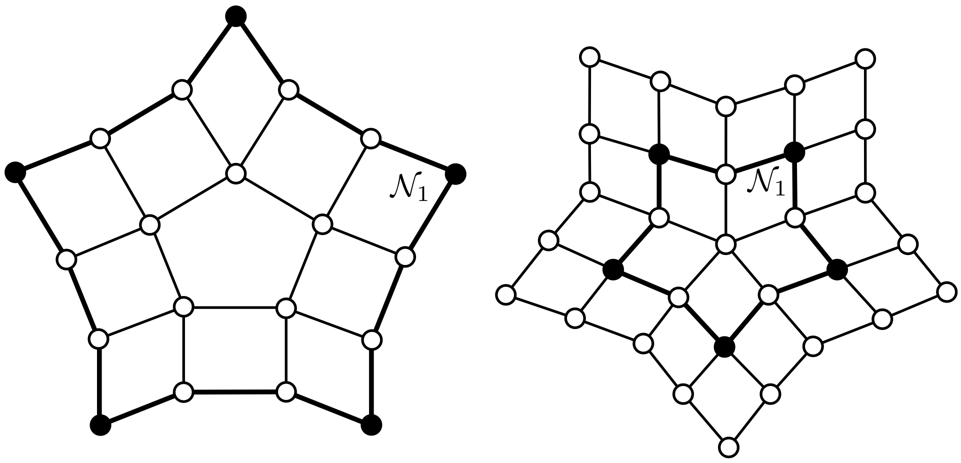

Figure 4.1: Examples of rings and ringnets: a 1-ringnet with an extraordinary face of valence 5 (left) and a 2-ringnet with an extraordinary vertex of valence 5 (right). The first rings $\mathcal{N}_1$ in both meshes are marked by bold lines and the convex corners of $\mathcal{N}_1$ are marked by $\bullet$.

Given a ringnet $\mathcal{N}$ and a generalized Catmull-Clark operator $U = \overline{M}_n$ of degree n, we generate the sequence $\mathcal{N}^{(l)} = U^l\mathcal{N}$.

Definition 4.1. (Ring and ringnet)
Let $\mathcal{N}_0$ be the subnet of $\mathcal{N}$ consisting of the extraordinary vertex or face of $\mathcal{N}$. The k-th ring around $\mathcal{N}_0$ is denoted by $\mathcal{N}_k$ and the mesh consisting of $\mathcal{N}_0, \ldots, \mathcal{N}_k$ by $\mathcal{N}_{0\ldots k}$. The latter is called a k-ringnet *or* k-net *for short. Furthermore, the submesh $\mathcal{N}_{i\ldots j}$ consists of $\mathcal{N}_i$, ..., $\mathcal{N}_j$.*

We say that a mesh $\mathcal{N}$ *influences* another subdivided mesh $\mathcal{M}$ if, during the subdivision, every vertex in $\mathcal{N}$ has an effect on some vertex in $\mathcal{M}$ and if additionally all vertices in $\mathcal{M}$ depend on $\mathcal{N}$.

In the definition of the smoothing operators $B_i = B_{\alpha_i,\beta_i}$, the parameter functions $\alpha_i(\cdot)$ and $\beta_i(\cdot)$ may have zero value, which means that, applying B_i on a ringnet $\mathcal{N}$, a generated vertex $\mathbf{v}_1$ or face $\mathbf{f}_1$ may be not influenced by some vertices in $\mathcal{N}$ that lie topologically in the direct neighborhood of $\mathbf{v}_1$ or $\mathbf{f}_1$. But, in fact, if we consider a whole step of $\overline{M}_n$, then, for a vertex $\mathbf{v}_2$ or face $\mathbf{f}_2$ of $\overline{M}_n\mathcal{N}$ with odd n or even n respectively, all vertices of $\mathcal{N}$ lying topologically in the direct neighborhood of $\mathbf{v}_2$ or $\mathbf{f}_2$ have an effect on $\mathbf{v}_2$ or $\mathbf{f}_2$ and there is a same influence relationship for $\overline{M}_n$ and M_n, where M_n is the midpoint scheme of degree n, due to the following lemma.

Lemma 4.2. (Same influence relationship for $\overline{M}_n$ and M_n)
Let $\mathcal{N}$ be a ringnet. For each pair of vertices in $\overline{M}_n\mathcal{N}$ and $M_n\mathcal{N}$ respectively, if n is odd, or for each pair of faces in $\overline{M}_n\mathcal{N}$ and $M_n\mathcal{N}$ respectively, if n is even, where they have the same topological location, these two vertices or faces are influenced by the same vertices in $\mathcal{N}$.

Proof. Since $\overline{M}_2 = M_2$ and $\overline{M}_{2r+2} = A\overline{M}_{2r+1}$, it suffices to consider $\overline{M}_n$ and M_n with odd degrees $n = 2r + 1$ over a primal or dual ringnet.

For $r = 1$, we see that every vertex $\mathbf{p}$ or face $\mathbf{f}$ of a primal or dual mesh $\mathcal{N}$ influences two subsets of vertices in $\overline{M}_3\mathcal{N}$ and $M_3\mathcal{N}$, when applying $\overline{M}_3\mathcal{N}$ and $M_3\mathcal{N}$ to $\mathcal{N}$, respectively, as shown schematically in Figure 4.2. And these two subsets of vertices have the same topological locations.

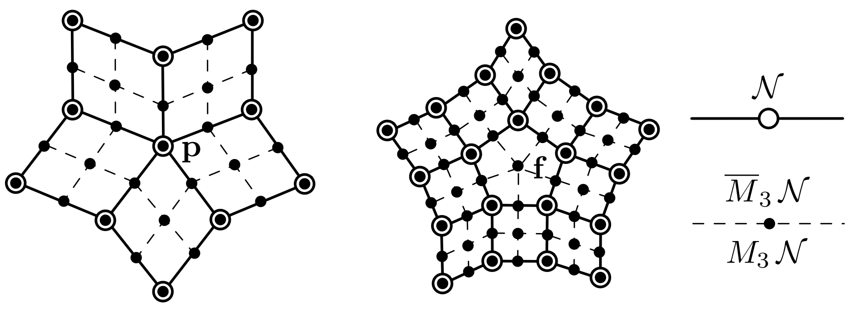

Figure 4.2: The vertices of $\overline{M}_3\mathcal{N}$ and $M_3\mathcal{N}$ which are influenced by an extraordinary vertex $\mathbf{p}$ (left) or an extraordinary face $\mathbf{f}$ (right) of valence 5.

Hence, this implies that the lemma is true for $\overline{M}_3$ and for $\overline{M}_4 = A\overline{M}_3$. By induction, it can be similarly shown that the lemma also holds for $\overline{M}_{2r+1}$ and $\overline{M}_{2r+2}$, $r \geq 2$. $\square$

Remark 4.3. (Core mesh)
The r-net $\mathcal{N}_{0\ldots r}$ of $\mathcal{N}$ consists of all vertices influencing $\mathcal{N}_0^{(l)}$ for some $l \geq 1$, where $r = \left\lfloor \frac{n-1}{2} \right\rfloor$. It is called the core (mesh) *of $\mathcal{N}$ with respect to U.*

Depending on the context, we treat any mesh as a matrix whose rows represent the vertices or as the set of all vertices.

It is straightforward to prove

Lemma 4.4. (Dependence after a subdivision step)
$\mathcal{N}_{0\ldots r+k}$ determines $\mathcal{N}^{(1)}_{0\ldots r+2k}$ for $k \geq 0$, i. e.,

$$\mathcal{N}^{(1)}_{0\ldots r+2k} = (U\,\mathcal{N}_{0\ldots r+k})_{0\ldots r+2k}\ .$$

If we subdivide just the regular parts of any $\mathcal{N}^{(k)}$, we obtain for every k a limiting surface $\mathbf{s}_k$. Since $\mathbf{s}_{k+1}$ contains $\mathbf{s}_k$, we can consider the difference surface $\mathbf{r}_k = \mathbf{s}_{k+1} \backslash \mathbf{s}_k$ whose control points are contained in a sufficiently large subnet $\mathcal{N}^{(k)}_{0\ldots\rho}$ with $\rho \geq n$ not depending on k. Due to Lemma 4.4, the operator U restricted to ρ-nets can be represented by a stochastic matrix $S = S_\rho$ called the *subdivision matrix*, i. e.,

$$\mathcal{N}^{(k+1)}_{0\ldots\rho} = S\,\mathcal{N}^{(k)}_{0\ldots\rho}\ . \tag{4.1}$$

Lemma 4.5. (Dependence property of a core mesh)
For some constant q depending on U and ρ, every vertex in $\mathcal{N}_{0\ldots r}$ influences all vertices in $\mathcal{N}^{(q+k)}_{0\ldots\rho} = (U^{q+k}\,\mathcal{N})_{0\ldots\rho}$ for all $k \geq 0$, which is denoted by

$$\mathcal{N}_{0\ldots r} \Rrightarrow \mathcal{N}^{(q+k)}_{0\ldots\rho}\ .$$

Proof. For sufficiently large l and any $k \geq 0$, every vertex in $\mathcal{N}_{0\ldots r}$ influences all vertices in $\mathcal{N}^{(l+k)}_0$, all vertices in $\mathcal{N}^{(l+k+1)}_{0\ldots 1}$, ..., and all vertices in $\mathcal{N}^{(l+k+\rho)}_{0\ldots\rho}$. Hence, we obtain the lemma with $q = l + \rho$. □

Theorem 4.6. (C^0-property of U)
The subdivision surfaces generated by U are C^0 continuous.

Proof. Since the subdivision matrix S is stochastic, i. e., S is a non-negative and real matrix and each row of S sums to 1, 1 is the dominant eigenvalue of S. Due to Lemma 4.5, there is an integer $l \geq 1$ such that

$$\mathcal{N}_{0\ldots r} \Rrightarrow \mathcal{N}^{(l)}_{0\ldots\rho} = S^l \mathcal{N}_{0\ldots\rho}\ .$$

This implies that S^l has a positive column and, according to [MP89, Theorem 2.1], any sequence $(S^i\,\mathbf{c})$ converges to a multiple of the vector $[1\ \ldots\ 1]^{\mathrm{t}}$ as $i \to \infty$ for all real vectors $\mathbf{c}$. Therefore, the only dominant eigenvalue of S is 1 and it has algebraic multiplicity 1.

Hence, the difference surfaces $\mathbf{s}_i \backslash \mathbf{s}_{i-1}$ converge to a point and the surfaces generated by U are continuous. □

To analyze the spectrum of the subdivision matrix S, we order any ρ-net $\mathcal{N}$ such that

$$\mathcal{N} = \begin{bmatrix} \mathcal{N}_{0\dots r} \\ \mathcal{N}_b \\ \mathcal{N}_a \\ \mathcal{N}_{r+2} \\ \vdots \\ \mathcal{N}_\rho \end{bmatrix} ,$$

where $\mathcal{N}_a$ consists of the convex corners and $\mathcal{N}_b$ of all other points in $\mathcal{N}_{r+1}$ (see Figure 4.1 for an illustration of the convex corners). With this arrangement, the subdivision matrix S has the lower triangular form

$$S = \begin{bmatrix} C & & & & & \\ * & B & & & & \\ * & * & A & & & \\ * & * & * & 0 & & \\ \vdots & & & \ddots & \ddots & \\ * & \dots & \dots & \dots & * & 0 \end{bmatrix} ,$$

where

$$\mathcal{N}^{(1)}_{0\dots r} = C\, \mathcal{N}_{0\dots r} \;, \tag{4.2}$$

$$\mathcal{N}^{(1)}_{b} = \begin{bmatrix} * & B \end{bmatrix} \begin{bmatrix} \mathcal{N}_{0\dots r} \\ \mathcal{N}_b \end{bmatrix} , \quad \text{and} \tag{4.3}$$

$$\mathcal{N}^{(1)}_{a} = \begin{bmatrix} * & * & A \end{bmatrix} \begin{bmatrix} \mathcal{N}_{0\dots r} \\ \mathcal{N}_b \\ \mathcal{N}_a \end{bmatrix} . \tag{4.4}$$

To verify this, we recall that any point influencing the core mesh influences $\mathcal{N}_0$ and thus belongs to the core mesh. This implies Equation (4.2) and shows that $\mathcal{N}_{r+1}$ influences only points in $(U\mathcal{N})_{r+1\dots\infty}$ and hence, that $\mathcal{N}_{r+2}$ influences only points in $(U\mathcal{N})_{r+2\dots\infty}$, etc. Since $\mathcal{N}_a$ does not influence any point in $\mathcal{N}^{(1)}_b$, Equations (4.3) and (4.4) follow. Moreover, due to Lemma 4.4, $(U\mathcal{N})_{r+2}$ is determined by $\mathcal{N}_{0\dots r+1}$ and $(U\mathcal{N})_{r+3}$ is determined by $\mathcal{N}_{0\dots r+2}$, etc.

Hence, the eigenvalues of S are zero or are the eigenvalues of the blocks C, B, and A.

Lemma 4.7. (Spectral radii of B and A)
The spectral radii ρ_B and ρ_A of B and A satisfy

$$\rho_B \leq \left(\frac{1}{2}\right)^{\lfloor \frac{n}{2} \rfloor + 1} \quad \textit{and} \quad \rho_A \leq \left(\frac{1}{4}\right)^{\lfloor \frac{n}{2} \rfloor + 1} .$$

In particular, it holds $\rho_B, \rho_A \leq 1/4$ for $n \geq 2$.

Proof. Since A is non-negative, we get [HJ85, Corollary 6.1.5 on Page 346]

$$\rho_A \leq \|A\|_\infty = \|A\mathbf{1}\|_\infty, \quad \text{where} \quad \mathbf{1} := [1 \ \dots \ 1]^{\mathrm{t}} .$$

The vector $A\mathbf{1}$ represents the convex corners of $\mathcal{N}_{r+1}^{(1)}$ if $\mathcal{N}_{0\dots r} = 0$, $\mathcal{N}_b = 0$, $\mathcal{N}_a = 1$, and $\mathcal{N}_{r+2\dots\rho} = 0$. One can easily verify that the (scalar-valued) vertices of these convex corners are

$$\frac{1}{4} \cdot \frac{1 - \alpha_1(4) - \beta_1(4)}{4} \cdot \dots \cdot \frac{1 - \alpha_r(4) - \beta_r(4)}{4} \quad \text{for } n = 2r+1 \text{ and}$$

$$\frac{1}{4} \cdot \frac{1 - \alpha_1(4) - \beta_1(4)}{4} \cdot \dots \cdot \frac{1 - \alpha_r(4) - \beta_r(4)}{4} \cdot \frac{1}{4} \quad \text{for } n = 2r+2.$$

Since $1 - \alpha_i(4) - \beta_i(4) \in (0, 1)$, this concludes the proof of the second statement. The first statement can be proved similarly. $\square$

5 The characteristic map

For the C^1 analysis of generalized Catmull-Clark subdivision, we need to investigate the eigenvectors and eigenvalues of the subdivision matrix S. We do this by subdividing special grid meshes as in [PC11] and recall the basic definitions in this section.

Definition 5.1. (Grid mesh)
A primal grid mesh *of valence m and frequency f is a planar primal ringnet with the vertices*

$$\mathbf{g}_{ij}^l = \begin{bmatrix} \mathrm{Re}(g_{ij}^l) \\ \mathrm{Im}(g_{ij}^l) \end{bmatrix} \in \mathbb{R}^2 ,$$

where $g_{ij}^l = ie^{\hat{\imath}2\pi lf/m} + je^{\hat{\imath}2\pi(l+1)f/m} \in \mathbb{C}$ and $i, j \geq 0$, $l \in \mathbb{Z}_m$, $\hat{\imath} = \sqrt{-1}$.
A dual grid mesh *of valence m and frequency f consists of the vertices*

$$\mathbf{h}_{ij}^l = \frac{1}{4}(\mathbf{g}_{i-1,j-1}^l + \mathbf{g}_{i,j-1}^l + \mathbf{g}_{i-1,j}^l + \mathbf{g}_{i,j}^l), \quad i, j \geq 1, \ l \in \mathbb{Z}_m$$

(see Figure 5.1). For fixed l, the vertices $\mathbf{g}_{ij}^l$ or $\mathbf{h}_{ij}^l$ with $(i, j) \neq (0, 0)$ of a grid mesh $\mathcal{N}$ build the l-th segment *of $\mathcal{N}$. The* segment angle *of $\mathcal{N}$ is $\varphi = 2\pi f/m$. The half-line from the center $\mathbf{g}_{00}^l$ through $\mathbf{g}_{10}^l$ is called the l-th* spoke*, denoted by $S_l(\mathcal{N})$ or S_l for short.*

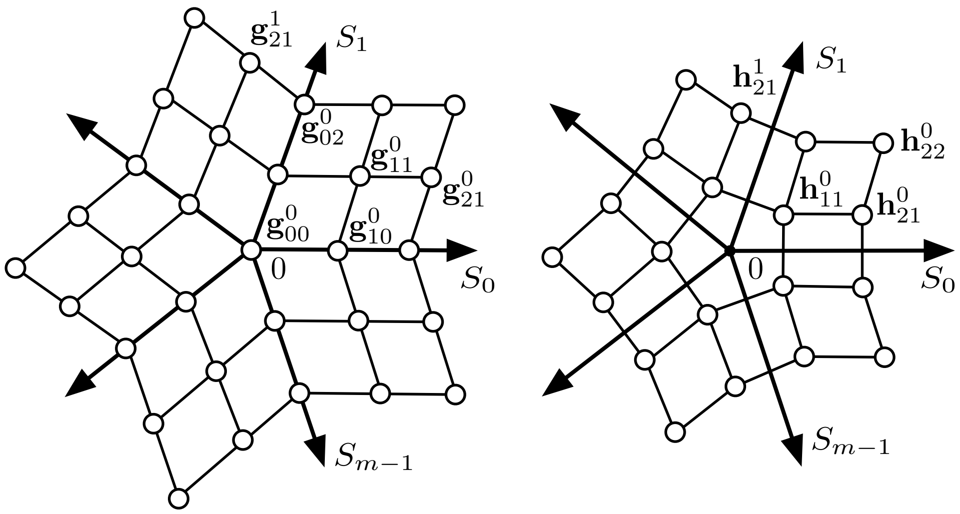

Figure 5.1: A primal grid mesh (left) and a dual grid mesh (right) with valence 5 and frequency 1.

Topologically, any ringnet $\mathcal{M}$ is equivalent to a grid mesh $\mathcal{N}$. Therefore, we use the same indices for equivalent vertices and denote the vertices of $\mathcal{M}$ by $\mathbf{p}^l_{ij}$.

Definition 5.2. (Symmetric ringnet)
A planar ringnet of valence m with the vertices $\mathbf{p}^l_{ij}$ in $\mathbb{R}^2$ is called rotation symmetric *with frequency f, if*

$$\mathbf{p}^{l+1}_{ij} = \begin{bmatrix} \cos\theta & -\sin\theta \\ \sin\theta & \cos\theta \end{bmatrix} \mathbf{p}^l_{ij} \quad \textit{with} \quad \theta = 2\pi f/m \; .$$

A planar ringnet $\mathcal{N} \in \mathbb{R}^2$ is called reflection symmetric *if its permutation $\widetilde{\mathcal{N}}$ consisting of the points $\widetilde{\mathbf{p}^l_{ij}} := \mathbf{p}^{(m-1)-l}_{ji}$ equals the conjugate ringnet $\overline{\mathcal{N}}$ consisting of the points*

$$\overline{\mathbf{p}^l_{ij}} = \overline{\begin{bmatrix} p^l_{ij,x} \\ p^l_{ij,y} \end{bmatrix}} = \begin{bmatrix} p^l_{ij,x} \\ -p^l_{ij,y} \end{bmatrix} ,$$

i. e.,

$$\widetilde{\mathcal{N}} = \overline{\mathcal{N}} \; .$$

A rotation and reflection symmetric ringnet is called symmetric*.*

Using the technique established in [PC11], we construct and analyze a characteristic map of a generalized Catmull-Clark scheme

$$U = B_r \cdots B_1 R \quad \text{or} \quad U = AB_r \cdots B_1 R$$

with $B_i = B_{\alpha_i,\beta_i}$. We follow [PC11] and use results stated there for midpoint subdivision that are also valid for generalized Catmull-Clark subdivision since their proofs are only based on the properties

(a) that the subdivision scheme preserves symmetry and generates midpoints or any convex combinations,

(b) due to Lemma 4.2, that midpoint schemes and generalized Catmull-Clark schemes have the same influence relationship when applying a whole subdivision operator, and

(c) that B_i maps a ringnet which is primal and rotation symmetric with frequency $f \neq 0$ to a ringnet of the same type and thus, B_i preserves the location of the extraordinary vertex.

Theorem 5.3. ($\mathcal{M}_\infty$ and λ_φ)
Let $\mathcal{M}$ be the core mesh of a grid mesh with frequency f and segment angle $\varphi := 2f\pi/m \in (0, \pi)$. Let

$$\mathcal{M}_k := \frac{(U^k\mathcal{M})_{0\ldots r}}{\|(U^k\mathcal{M})_{0\ldots r}\|} ,$$

where $\|\cdot\|$ denotes any matrix norm. Then the following statements hold.

(a) The sequence $(\mathcal{M}_k)_{k\in\mathbb{N}}$ converges to a symmetric eigennet $\mathcal{M}_\infty$ with segment angle φ and a positive eigenvalue λ_φ, which depends only on φ but not on f and m. $(\mathcal{M}_\infty)_{0\ldots 1}$ has at most one zero control point. Additionally, we define $\lambda_\pi = |\gamma_\pi|$, where γ_π is the maximum eigenvalue associated with a rotation symmetric eigenvector with segment angle π.

(b) Restricting U to the core meshes, the eigenvalue λ_φ is the dominant eigenvalue of the eigenspaces of frequencies f and $m - f$ and it has geometric and algebraic multiplicity 2.

(c) $\lambda_\alpha > \lambda_\theta > \lambda_\pi$ for $0 < \alpha < \theta < \pi$.

This can be proved as (5.4), (5.7), (6.3), and (6.4) in [PC11]. For midpoint subdivision schemes for quadrilateral meshes, λ_π is equal to 1/4 and to the subdominant eigenvalue μ_0 of frequency 0. This implies that $\lambda_{2\pi/m}$ is subdominant. However, for a generalized Catmull-Clark subdivision scheme, λ_π can be smaller than μ_0. Therefore, we use the following lemma to show that $\lambda_{2\pi/m}$ is subdominant for $m > 4$.

Lemma 5.4. ($\lambda_{\pi/2} = 1/2$)

(a) For $m = 4$, the operator U has the subdominant eigenvalue $1/2$.

(b) $\lambda_{\pi/2} = 1/2$ holds for any m and f such that $\frac{2f\pi}{m} = \frac{\pi}{2}$.

Proof. We consider a regular scalar-valued eigenmesh $\lambda\mathcal{M} = U\mathcal{M}$ with eigenvalue λ. Since

$$\lambda\mathcal{M}_{\nabla\nabla} = U_{\nabla\nabla}\mathcal{M}_{\nabla\nabla}$$

and $\|U_{\nabla\nabla}\| < 1/2$ due to Lemma 3.2, it follows that $|\lambda| < 1/2$ or that $\mathcal{M}_{\nabla\nabla} = 0$, meaning that $\mathcal{M}$ is a linear image of a regular grid $\mathcal{G}$, i.e., a linear combination of the constant mesh $[1\ \dots\ 1]^{\mathrm{t}}$ with eigenvalue 1 and the two coordinates of $\mathcal{G}$. Since $U\mathcal{G} = \frac{1}{2}\mathcal{G}$, (a) follows for $m = 4$. Since there is a basis of rotation symmetric eigenmeshes, it suffices for $m \neq 4$ to consider a rotation symmetric mesh $\mathcal{M}$ with segment angle $\pi/2$. Due to symmetry, the subdivided mesh $U\mathcal{M}$ does not depend on f, whence (b) follows. $\square$

We observe two ringnets of frequency 0 with different valencies m_1 and m_2. If their first segments and their extraordinary vertices or the vertices on the extraordinary faces are identical, respectively, then the generated first segments and the generated extraordinary vertices or the vertices on the generated extraordinary faces are also identical after applying R or $B_{\alpha,\beta}$ or A if $\alpha(m_1) = \alpha(m_2)$ and $\beta(m_1) = \beta(m_2)$. Hence, we get

Lemma 5.5. ($\lambda_{2\pi/m}$ **and** μ_0)
For constant functions $\alpha_1, \beta_1, \dots, \alpha_r, \beta_r$, the subdominant eigenvalue μ_0 of frequency 0 does not depend on valence m and hence

$$|\mu_0| \leq 1/2 = \lambda_{\pi/2} < \lambda_{2\pi/m}$$

for $m \geq 5$ due to Lemma 5.4 and Theorem 5.3 (c).

Lemmas 5.4 and 5.5 together with Theorem 5.3 and Lemma 4.7 can be used as in the proof of Theorem (7.3) in [PC11] to derive the following corollary.

Corollary 5.6. (Subdominant eigenvalue for $m \geq 5$)
Let ρ be as in Equation (4.1) and let U be a generalized Catmull-Clark subdivision operator of degree n mapping the space of ρ-ringnets of valence m to itself with constant functions $\alpha_i, \beta_i \in [0, 1)$, $n \geq 2$, and $1 - \alpha_i - \beta_i \in (0, 1)$. Let $\mathcal{M}$ be a ρ-grid mesh of valence m and frequency 1. If $m \geq 5$, the meshes

$$\mathcal{M}_k := \frac{U^k\mathcal{M}}{\|U^k\mathcal{M}\|}$$

converge to a subdominant eigenmesh $\mathcal{M}_\infty$ of U called the characteristic mesh *of U and its eigenvalue $\lambda_{2\pi/m}$ has geometric and algebraic multiplicity 2.*

Remark 5.7. (Subdominant eigenvalue for $m = 3$ and for U with non-constant functions α_i and β_i)
Corollary 5.6 is true for $m = 3$ if

$$\lambda_{2\pi/m} > \max\{|\mu_0(m)|, \rho_B, \rho_A\} \tag{5.1}$$

and Corollary 5.6 is also true for U with non-constant functions α_i, β_i and $m \geq 5$ if

$$\lambda_{2\pi/m} > |\mu_0(m)| \ , \tag{5.2}$$

where ρ_B and ρ_A are the spectral radii defined in Lemma 4.7.

6 Smoothness for irregular meshes

Let $\mathcal{C}$ be the characteristic mesh of valence m of the generalized Catmull-Clark scheme

$$U = B_r \cdots B_1 R \quad \text{or} \quad U = AB_r \cdots B_1 R$$

with $B_i = B_{\alpha_i,\beta_i}$, $\alpha_i, \beta_i \in [0, 1)$, and $1 - \alpha_i - \beta_i \in (0, 1)$. It defines the control mesh of a characteristic map, which is a surface ring consisting of m segments.

Theorem 6.1. (C^1-property of U_n)
The generalized Catmull-Clark scheme $U = \overline{M}_n$ of degree $n \geq 2$ with constant functions α_i, β_i is a C^1 subdivision algorithm for valencies $m \geq 5$. U is also a C^1 algorithm with non-constant functions α_i, β_i or for $m = 3$ if Inequality (5.2) or Inequality (5.1) is satisfied, respectively.

Proof. To simplify the notation, we identify the real plane $\mathbb{R}^2$ with the complex plane $\mathbb{C}$ by the bijection $\mathbb{R}^2 \ni [x\ y]^{\mathrm{t}} \mapsto x + \hat{\imath} y \in \mathbb{C}$. Let $\mathbf{c}(x, y) : \Omega \to \mathbb{C}$ be 3 segments of the characteristic map of U, where $\Omega = \Omega_{-1} \cup \Omega_0 \cup \Omega_1$ as shown at the left of Figure 6.1, and $\mathbf{c}_{|\Omega_i}$ is the i-th segment for $i = -1, 0, 1$.

First, we observe a grid mesh $\mathcal{M}$ as shown at the right of Figure 6.1 such that the subdivided and normalized meshes $\mathcal{M}_k = (U^k\mathcal{M})_{0\ldots\rho}/\|(U^k\mathcal{M})_{0\ldots\rho}\|$ converge to the characteristic mesh $\mathcal{C}$ due to Corollary 5.6 and Remark 5.7. If n is odd, we require $\mathcal{M}$ to be primal and otherwise to be dual. Let $\mathcal{E}_k = \nabla_2(\mathcal{M}_k)$ and $\mathcal{E} = \nabla_2(\mathcal{C})$, where the edge set of a ringnet $\mathcal{K} = [\mathbf{p}^k_{ij}]$ is defined by

$$\nabla_2(\mathcal{K}) := \{\nabla_2 \mathbf{p}^0_{i,j} = \mathbf{p}^0_{i,j} - \mathbf{p}^0_{i,j-1} \mid i \geq 0, j > 0\} \ ,$$

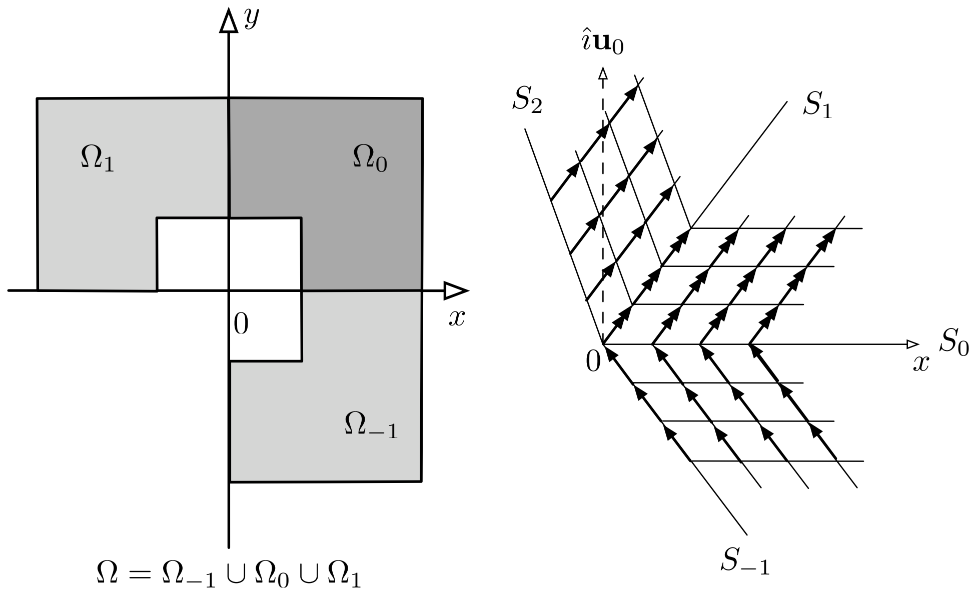

Figure 6.1: The domain Ω of $\mathbf{c}$ (left) and the -1, 0, 1-th segments of a grid mesh (right), where the y-edges in the three segments are marked by arrows and the y-edges in the 0-th segment are especially marked by double arrows.

as illustrated at the right of Figure 6.1. These and other edges control the directions of the partial derivatives $\mathbf{c}_y(\Omega_0)$. Furthermore, we add both $\mathbf{u}_1$ and $\hat{\imath}\mathbf{u}_0$ to $\mathcal{E}_k$ and $\mathcal{E}$, where $\mathbf{u}_1$ is the edge direction of the spoke S_1 and $\hat{\imath}\mathbf{u}_0$ is the edge direction of the spoke S_0 rotated by $+\pi/2$. Refining, averaging, and smoothing a mesh also means its edges are averaged by the masks shown in Figure 6.2. In particular, the edges in $\mathcal{E}_k$ are either, due to symmetry, parallel to $\mathbf{u}_1$ and $\hat{\imath}\mathbf{u}_0$ or obtained by iteratively averaging the edges in $\mathcal{E}_{k-1}$ and multiplying these by positive numbers because of the normalization. Thus, we know that $\mathcal{E}_k$ lies in the cone spanned by $\mathcal{E}_{k-1}$, i. e., in the cone

$$\mathcal{D}_0 := \begin{cases} [0,\infty)\, e^{\hat{\imath}[\pi/2,\, 2\pi/3]} & , \text{ if } m = 3 \\ [0,\infty)\, e^{\hat{\imath}[2\pi/m,\, \pi/2]} & , \text{ if } m \geq 5 \end{cases} .$$

Therefore, by induction, all $\mathcal{E}_k$ and $\mathcal{E}$ lie in $\mathcal{D}_0$.

Moreover, since $\mathcal{C}_{0\ldots1}$ is symmetric and has at most one zero control point, at least one of its edges is non-zero. Subdividing $\mathcal{C}$, we can see that every element of $\mathcal{E}$ is a linear combination of $\mathcal{E}$ with non-negative weights and a positive weight for the non-zero element in the 1-ringnet. Hence, $\mathcal{E}$ has no zero elements.

Second, we observe that for a symmetric ringnet $\mathcal{N}$, each element of

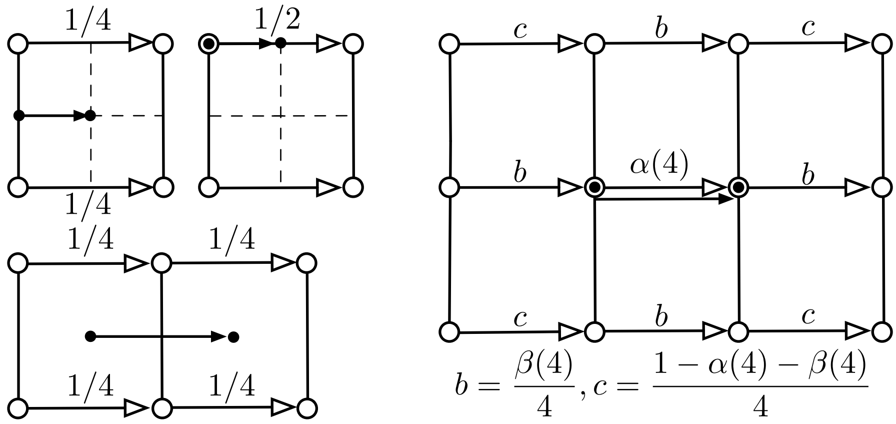

Figure 6.2: Masks for R_∇ (top left), A_∇ (bottom left), and $(B_{\alpha,\beta})_\nabla$ (right) on regular meshes.

$\nabla_2(2R\mathcal{N})$, $\nabla_2(A\mathcal{N})$, and $\nabla_2(B_{\alpha,\beta}\mathcal{N})$ is a convex combination of elements in $\nabla_2(\mathcal{N})$, in $\nabla_2(\mathcal{N})$ reflected at S_1, and in $-\nabla_2(\mathcal{N})$ reflected at S_0, where a reflected element has a smaller weight than its unreflected counterpart. Thus, by induction, we see that $\nabla_2(2^k U^k \mathcal{C}) \subset \mathcal{D}_0$, for $k \geq 0$. Since every partial derivative $\mathbf{c}_y$ over Ω_0 is the limit of a sequence of vectors $\mathbf{v}_k \in \nabla_2(2^k U^k \mathcal{C})$, it follows that $\mathbf{c}_y(\Omega_0) \subset \mathcal{D}_0$.

Next, we show $\mathbf{0} \notin \mathbf{c}_y(\Omega_0)$. Any $\mathbf{c}_y(\mathbf{x})$, $\mathbf{x} \in \Omega_0$, is a convex combination of $\mathcal{F}_{-1}$ or $\mathcal{F}_0$, where $\mathcal{F}_i$ is the set of all y-edges in the segments i and $i+1$ of $2^k U^k \mathcal{C}$ for sufficiently large k. We observe

$$\mathcal{F}_{-1} = e^{\pi/2 - 2\pi/m} \mathcal{F}_0 \subseteq \begin{cases} (0,\ \infty)\, e^{\hat{\imath}[\pi/3,\ 2\pi/3]} & , \quad \text{if } m = 3 \\ (0,\ \infty)\, e^{\hat{\imath}[2\pi/m,\ \pi - 2\pi/m]} & , \quad \text{if } m \geq 5 \end{cases},$$

which implies $\mathbf{0} \notin \mathbf{c}_y(\Omega_0)$. Hence, $\mathbf{c}_y(\Omega_0) \subset \mathcal{D} := \mathcal{D} \backslash \{\mathbf{0}\}$ and similarly $\mathbf{c}_x(\Omega_0) \subset \mathcal{D} - \pi/2$.

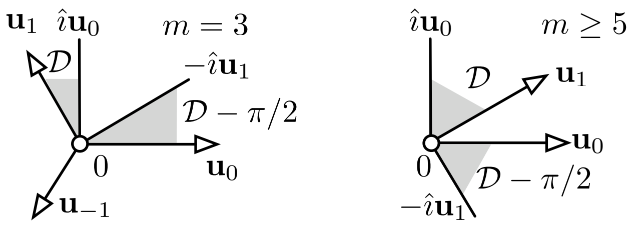

Figure 6.3: The direction cones $\mathcal{D}$ and $\mathcal{D} - \pi/2$.

Since each element of $\mathcal{D}$ is linearly independent with each element of $\mathcal{D} - \pi/2$ (see Figure 6.3), $\mathbf{c}$ is regular over Ω_0 and hence, the total characteristic map of U is regular. Because $\mathbf{c}_y(\Omega_0) \subset \mathcal{D}$, $\mathbf{c}$ does not map any line segment between two points in Ω_0 to a closed curve, meaning that $\mathbf{c}$ is injective over Ω_0. Moreover, since $\mathcal{M}$ is a symmetric grid mesh whose zeroth segment lies in $[0,\ \infty)\ e^{\hat{\imath}[0,\, 2\pi/m]} =: \mathcal{A}$ and U preserves symmetry, it implies $\mathbf{c}(\Omega_0) \subset \mathcal{A}$ and $\mathbf{c}$ maps the interior of Ω_0 into the interior of $\mathcal{A}$. Hence, the total characteristic map of U is injective. Finally, Reif's C^1-criterion [Rei95, Theorem 3.6] is satisfied, which concludes the proof. $\square$

Example 6.2. ($\overline{M}_3$)
For $U = B_{\alpha,\beta}R$ with $\alpha, \beta \in [0,1)$, $1-\alpha-\beta \in (0,1)$ and for valence m, applying the discrete Fourier transform *on the subdivision matrix of $\overline{M}_3$, we get*

$$\mu_0(m) = \frac{3\alpha(m) + \beta(m) + \sqrt{(3\alpha(m) + \beta(m))^2 - 4t\,\alpha(m)}}{8}$$

and

$$\lambda_{\frac{2\pi}{m}}(m) = \frac{4 + t + (2-t)c + \sqrt{(2-t)^2c^2 + 2(4+t)(2-t)c + (4-t)^2}}{16},$$

where $t = 2\alpha(4) + \beta(4)$ and $c = \cos(2\pi/m)$. According to Theorem 6.1, if $\alpha(m) = \alpha(4)$, $\beta(m) = \beta(4)$, and $m \geq 5$, then $\overline{M}_3$ generates C^1 surfaces around extraordinary points of valence m. Otherwise, $\overline{M}_3$ generates C^1 surfaces around extraordinary points of valence m if $\lambda_{\frac{2\pi}{m}}(m) > \mu_0(m)$ holds, since it can be easily verified that

$$\lambda_{\frac{2\pi}{m}}(m) \geq \frac{5}{16} > \frac{1}{4} \geq \max\{\rho_A,\ \rho_B\}\ .$$

7 Conclusion

In this paper, a new class of generalized Catmull-Clark subdivision schemes is introduced and the smoothness of the resulting subdivision surfaces is analyzed. The established C^1 analysis tools for quadrilateral meshes in [PC11] have been generalized to the convex combination operator $B_{\alpha,\beta}$. Furthermore, a deeper understanding of the spectral properties of the subdivision matrices at extraordinary points is provided.

Tools to analyze wider and infinite classes of subdivision schemes are developed in this paper and hopefully help to advance the state of the art towards general C^1 analysis tools for other subdivision schemes that can be factorized into general and simple convex combination operators.

References

[CC78] Edwin Catmull and Jim Clark. Recursively generated B-spline surfaces on arbitrary topological meshes. *Computer-Aided Design*, 10(6):350–355, November 1978.

[DS78] Daniel W. H. Doo and Malcolm A. Sabin. Behaviour of recursive division surfaces near extraordinary points. *Computer-Aided Design*, 10(6):356–360, November 1978.

[Dyn92] Nira Dyn. Subdivision schemes in computer-aided geometric design. In Will A. Light, editor, *Advances in Numerical Analysis II, Wavelets, Subdivision algorithms, and Radial Basis Functions*, pages 36–104. Clarendon Press, Oxford, 1992.

[HJ85] Roger A. Horn and Charles R. Johnson. *Matrix analysis*. Cambridge University Press, first published edition, 1985.

[Kob00] Leif Kobbelt. $\sqrt{3}$-subdivision. In *Proceedings of SIGGRAPH 2000, Computer Graphics Proceedings, Annual Conference Series. ACM*, pages 103–112, 2000.

[LR80] Jeffrey M. Lane and Richard F. Riesenfeld. A theoretical development for the computer generation and display of piecewise polynomial surfaces. *IEEE Transactions on Pattern Analysis and Machine Intelligence*, 2(1):35–46, January 1980.

[MP89] Charles A. Micchelli and Hartmut Prautzsch. Uniform refinement of curves. *Linear Algebra and its Applications*, 114/115:841–870, 1989.

[PC11] Hartmut Prautzsch and Qi Chen. Analyzing midpoint subdivision. *Computer Aided Geometric Design*, 28(7):407–419, 2011.

[PR98] Jörg Peters and Ulrich Reif. Analysis of algorithms generalizing B-spline subdivision. *SIAM Journal on Numerical Analysis*, 35(2):728–748, 1998.

[Rei95] Ulrich Reif. A unified approach to subdivision algorithms near extraordinary vertices. *Computer Aided Geometric Design*, 12:153–174, 1995.

[ZS01] Denis N. Zorin and Peter Schröder. A unified framework for primal/dual quadrilateral subdivision schemes. *Computer Aided Geometric Design*, 18(5):429–454, June 2001.